Journal of Materials Science: Materials in Engineering

ORIGINAL PAPER Open Access

Screening the efficacy of platinum-based nanomaterial synthesized from *Allium sativum* to control plant pathogens

Dhanushwr Kumar[1†], Ranjani Soundhararajan[1†] and Hemalatha Srinivasan[1*]

Abstract

Emerging challenge posed by multidrug-resistant *Bacillus* spp. phytopathogens on agriculture and their commodities exerts pressure on global food security. This mandates the search for other alternatives to existing antibiotics. This study reports a novel method of green synthesis of platinum nanoparticles (PtHGNM) using aqueous extract of Himalayan garlic (*Allium sativum*). Physicochemical characterization techniques including UV-visible spectrometry, FT-IR, XRD, DLS, zeta potential, and FESEM-EDAX disclosed the biogenic fabrication of a stable and amorphic nano platinum material. This nanoparticle exhibited high bactericidal efficacy and effectively inhibited biofilm formation by the model plant-borne pathogens used in this study. We estimated the membrane integrity, oxidative enzymes and stress parameters of bacteria to elucidate the underlying mechanism of action of PtHGNM. This research uncovered the potential of biogenic nanoparticles for sustainable plant disease management and paved the way for further analysis of its properties and mechanism of its action.

Keywords Multidrug resistant, *Bacillus* spp., Himalayan garlic, Platinum nanoparticles, High bactericidal efficacy

Introduction

With an array of exceptional properties including mechanical, chemical, optical and magnetic, noble metals are highly inquired for diverge range of applications. But dependance on highly reactive synthetic chemical substances: sodium borohydride and hydrazine during traditional methods for metallic nanoparticles synthesis leads to severe ecological challenges. These toxic chemicals restrict their broad spread utilization and call for comprehensive safeguard measures to protect the environment (Gautam et al. 2021; Pandit et al. 2022).

Plant extracts pose a much greener and constructive option for synthesis of metallic or any other specific metallic oxide nanoparticles. This cultivates an environmentally sound, economically viable, and efficient process by harnessing naturally available bio-reducing properties of the plants. By wielding the solar energy, plants offer a sustainable, renewable and yet an appealing biological process that eliminates expensive energy inputs required when compared to techniques that are either enzymatic, microbes mediated or any others. Plants also abound antioxidants, sugars and other biomolecules that act as key elements influencing nanoparticle formation. Their extracts serve as valuable and robust asset for researchers to unravel any multifaceted processes that govern the green synthesis of either metallic or metallic oxide nanoparticles. It also provides glimpse into complex and innate abilities of biomolecules to reduce, nucleate and stabilize nanoparticles (Kaningini et al. 2022; Shafey 2020).

[†]Dhanushwr Kumar and Ranjani Soundhararajan contributed equally to this work.

*Correspondence:
Hemalatha Srinivasan
hemalatha.sls@bsauniv.ac.in
[1] School of Life Sciences, B.S. Abdur Rahman Crescent Institute of Science and Technology, Vandalur, Chennai 48, India

Through investigating plant-mediated mechanisms, researchers can comprehend the intricates that shape nanoparticles form, size and surface attributes. This knowledge is crucial since it helps in optimizing the green synthesis protocols and to employ these nanoparticles for definite applications. Academically, rigorous research efforts centred around metal nanoparticles, specifically with materials like manganese, copper dioxide and oxides of zinc, titanium, cerium, copper, ferric and calcium, are being actively studied (Chopra et al. 2022; Salem and Fouda 2021; Vijayaram et al. 2024). During the initial investigations, scientists utilized plant extracts sourced from diverse range of plant sources. One aspect observed in the early explorations is that not only the specific plant extract but also the plant part that was used for the extract also profoundly influenced the characteristics of the nanoparticles. Intriguingly, plant extracts can able to diminish the intrinsic toxicity of the nanoparticles as well. These bio fabrication methods are also recognized for their remarkable efficiency in forming nanoparticles with desirable attributes. Synthesis of nanoparticles employing noble metals like gold, silver and copper through implementation of biomimetic strategies demonstrated effectiveness of biomolecular actions. Platinum, a transition metal of immense value, possesses a remarkable potential. Platinum nanoparticles exhibit formidable effectiveness and stands out as a promising candidate for antimicrobial agents (Eltaweil et al. 2022; Faisal et al. 2024; Jan et al. 2021). Due to lack of scientific knowledge regarding green synthesis of platinum nanomaterials, it presents us with significant prospect to explore and develop pioneering biological techniques that lends controllable biogenic fabrication of productive and biocompatible platinum nanoparticles (Behzad et al. 2021; Malode et al. 2023).

Single clove Himalayan garlic (*Allium sativum*) is a rare wild garlic cultivar, endemic and indigenous to Himalayan regions of India (Kaur et al. 2023). It is also known by Snow Mountain garlic or Kashmiri garlic. This garlic variety can be morphologically distinguished by a single-, small-, pointed- and pearl-shaped bulb with a tough golden-brown sheath. It grows in harsh Himalayan climate, tolerating subzero temperatures (as low as −10 °C), severe hypoxic conditions, and can thrive in the altitudes exceeding 6000 m (Mehra et al. 2020). Apart from being resilient to environmental challenges, it held a prominent position for its potential medicinal properties. It possesses pharmacological functions for different conditions, including hypertension, atherosclerosis, diabetes and cancer (Mehra et al. 2020; Terán-Figueroa et al. 2022). It also corroborates immunomodulatory activity, by regulating immune function. Studies indicate that garlic grown at higher altitudes shows a sevenfold rise in organosulfur content, which could potentially increase its claimed therapeutic benefits (Mehra et al. 2020). Due to limited attention from scientific community, data on single-clove Himalayan garlic remains scarce, despite its promising therapeutic potential and traditional applications. This garlic requires further research exploring the unique properties and also regarding its phytocompounds and the efficacy of reported therapeutic properties.

We aim to study and gain insights about biogenically fabricated platinum nanoparticles using snow mountain garlic extract. We believe that this Himalayan garlic-mediated platinum nanoparticles (PtHGNM) will potentially act as a bactericide against *Bacillus* spp. phytopathogens isolated from the cardamom, coffee and pepper plant. Several biochemical investigations will be implemented to understand the mechanism of possible antibacterial action. Furthermore, PtHGNM toxicity profile will also be evaluated to ensure its safety for future applications.

Methodology

Aqueous extraction and phytochemical screening of Himalayan garlic

Fresh single whole cloves of the snow mountain garlic were peeled, sterilized and ground into smooth paste using a blender. Aqueous extract of 10% w/v is prepared by macerating 30 g of the freshly ground paste into 300 mL of autoclaved distilled water overnight at 37 °C under constant agitation using orbital shaking incubator. With Whatman grade 1 filter paper, the extract was strained, and the filtrate obtained was kept at 4 °C for further analysis. The filtrate was then qualitatively assessed for phytochemical compounds. Tests for alkaloids, carbohydrates, reducing sugars, glycoside, proteins, amino acids, flavonoids, phenols, saponins, terpenoids, triterpenoids, and steroids were carried out following the method of Harborne (1973).

Biogenic fabrication and physicochemical characterization of platinum nanoparticles

Initially, a reaction of mixture was made of one part of the garlic extract filtrate to nine parts of platinum precursor: 1-mM hexachloroplatinic acid hexahydrate solution. This mixture was maintained in normal room conditions and visually observed throughout the day. Bioreduction of platinum was affirmed by the formation of a settlement. Then it was subjected to centrifugation for about quarter of an hour at 8000 rpm under 4 °C. The pellet obtained was washed subsequently with sterile water, thrice and with 70% ethanol to eradicate any residual contaminants. Finally, after washing the pellet with Milli-Q water, it was dried in hot air oven maintained at 60 °C,

yielding PtHGNM. When required for the analysis, the dried nanoparticles were sonicated to disperse them in water.

Synthesis of PtHGNM was primarily examined using UV-visible spectroscopy. After confirming the synthesis by exhibition of a characteristic surface plasmon resonance (SPR) peak at 228 nm, comprehensive set of analytical methods were employed to study about the functional groups, form, composition, structure, dimensions and stability of the nanoparticle via Fourier transform infrared spectroscopy (FT-IR), X-ray diffraction (XRD), field-emission scanning electron microscopy-energy-dispersive X-ray spectroscopy (FESEM-EDAX), dynamic light scattering (DLS) and zeta-potential analysis.

In vitro phytotoxicological evaluation of PtHGNM on *Vigna radiata*

Seed germination was assessed as outlined by Anwar et al. (2021), with appropriate modifications to understand the effects of PtHGNM. Sequential surface sterilization was carried out on healthy *V. radiata* (mung bean) seeds by initially immersing in 70% ethanol for 5 min and 1% sodium chloride solution for 1 min, followed by rinsing them with sterile distilled water. Different test concentrations: 7.8, 15.6, 31.2 and 62.5 µg/mL prepared by serially diluting PtHGNM stock solution 500 µg/mL in distilled water were allowed to be exposed to the seeds. A control group received only distilled water. For 2 days and under ambient temperature, germination was monitored in triplicate petri dishes, each containing six seeds. The number of germinated seeds relative to the total number of seeds sown was noted to estimate the germination percentage. Following germination analysis, the seedlings were transplanted into seedling trays containing red soil. Each well was planted with six seedlings and performed in triplicates. Four PtHGNM test concentrations including 7.8, 15.6, 31.2 and 62.5 µg/mL prepared in distilled water were used for daily treatments (200 µL/well). A control group received only distilled water. The experiment was conducted for a duration of 5 days under controlled light conditions at 37 °C. Various developmental parameters were measured randomly on both treated and control plants after the treatment period. These included the fresh weight of the entire plant and the root and stem lengths of individual seedlings.

In vitro toxicological evaluation of PtHGNM on *Danio rerio* embryos

The impact of PtHGNM on zebrafish (*D. rerio*) embryo development was assessed as per OECD (Organization for Economic Cooperation and Development) test guideline 236. Wild-type zebrafish eggs were collected from group spawning. Healthy embryos were selected, washed gently with embryo media (1×E3 medium) and distributed to 24-well plates within 2 hpf (hours post-fertilization). Each well contained 5 embryos in 2 mL of 1×E3 media supplemented with respective PtHGNM concentration (1, 5, 10, 20, 30, 40, 50 and 60 µg/mL) prepared by dilution of the stock solution (500 µg/mL) in E3 media. A control group received only E3 media. The experiment was conducted in triplicate, with each concentration tested with 15 embryos. A total of 135 embryos were used, including tests and control. Static test method was executed, and throughout the experiment (96 hpf), the embryos were continuously exposed to their respective treatments. At 24, 48, 72 and 96 hpf, developmental parameters were monitored. These included mortality, coagulation of embryos, somite formation, detachment of the tail bud from the yolk sac, hatching rate, touch response and finally heart rate. The percentage of embryos hatched after 72 hpf was calculated. At each observation time point, embryo heartbeats were directly counted for 5 s and converted to beats per minute. The average heart rate was determined for each concentration group. Finally, to assess the larvae's touch response, the outer margins of the trunk were delicately palpated using a smooth pipette tip. The incubation temperature was maintained at a constant 27 °C throughout the experiment.

Isolation and phylogenetic analysis of plant pathogenic bacteria

Coffee, cardamom and pepper leaves exhibiting characteristic disease symptoms were collected from Kodagu (Coorg) district located in eastern declivities of Western Ghats, India. Symptomatic tissues were dissected aseptically into small pieces and plated on Luria-Bertani (LB) agar for 24 h at 37 °C. Discrete colonies with salient morphologies were isolated, purified through repeated streaking and grown in LB broth for DNA isolation by heat lysis technique. The DNA extracted served as a template for amplifying the 16S rRNA gene using the universally established primers: 27F and 1492R (Soundhararajan et al. 2023). Final products of the PCR were purified and underwent Sanger sequencing for identification of the plant-associated pathogenic bacterial species. After identification, phytopathogens screened for their susceptibility towards various antibiotics using disc diffusion technique. Phylogenetic tree was drawn using MEGA X software and an online server, iTOL, among the isolated model organisms and closely related species. BLAST program was utilized to identify highly similar species. Finally, neighbour joining trees were constructed via MUSCLE program.

Antibacterial and antibiofilm activity of PtHGNM

The antibacterial activity of the PtHGNM were evaluated as per Ranjani et al. (2020) using microtitre plate. Initially, all the wells were filled with Luria-Bertani broth, serially diluted with nanoparticles. The test concentration included was 500, 250, 125, 62.5, 31.25, 15.63, 7.81 and 3.91 µg/mL. Bacterial culture was then inoculated into respective wells. Both positive and negative control groups were included for comparison. Positive control group with broth, ampicillin (1 mg/mL), bacterial cultures and negative control group with only broth and bacterial cultures were maintained. During the period of incubation, the samples were monitored visually for the degree of turbidity. The minimum inhibitory concentration (MIC) of PtHGNM was evaluated as the sample with the least concentration appeared with no visible growth. The minimum bactericidal concentration (MBC) was examined as per Ranjani et al. (2020), based on the lowest concentration of PtHGNM needed to entirely hinder the colony formation on agar plates. After MIC estimation, smaller aliquots from all the wells with no visible growth, i.e. the MIC well as well as the subsequent wells with higher concentrations of PtHGNM, were plated onto LB agar. Following the incubation, the treatment concentration that resulted in zero colony formation and growth was defined as MBC. Estimation of antibiofilm activity (Ranjani et al. 2020) of PtHGNM was executed as same as MIC determination. After the incubation period, the contents of the plates were discarded cautiously. Afterwards, the plates were rinsed with sterile water and dried. All of the wells received 0.1% crystal violet solution treatment, followed by 15-min incubation at room conditions. Plates were inverted carefully to discard the stain and rinsed with sterile distilled water again. Then the plates were placed inverted on sterile paper towels to completely get rid of all the residual stain. Finally, to measure the biofilm formation, all the wells were treated with 30% glacial acetic acid and incubated for 10 min with constant agitation to facilitate the crystal violet stain solubilization. Absorbance was recorded at 595 nm.

PtHGNM-mediated disruption of membrane integrity in phytopathogens

The effects of PtHGNM treatment on the membrane permeability of bacterial cultures were evaluated based on previously established techniques. As markers of membrane integrity, both protein and sugar leakage from the cells were measured (Liu et al. 2022a). The concentration of PtHGNM was adjusted to the minimum inhibitory concentrations (MICs) found for each bacterial species. The test method includes two control groups: a positive control subjected to ampicillin and a negative control without any sort of intervention. The cultures were then shaken while being maintained at 37 °C for 4 h. Aliquots of all cultures were centrifuged at 10,000 rpm for 30 min at 4 °C. The supernatants obtained were preserved at −20 °C further until protein and sugar content analysis.

PtHGNM-mediated manipulation of antioxidant system in phytopathogens

The PtHGNM antiradical effects have been assessed by the measurement of malondialdehyde (MDA) production, a lipid peroxidation biomarker, utilizing the thiobarbituric acid-reactive substance (TBARS) assay (Heath and Packer 1968). Bacterial cultures treated with PtHGNM according to their respective MICs. This study was examined with two control groups including a positive control that received ampicillin and a negative control without any form of treatment. The cell suspensions were centrifuged (10,000 rpm, 30 min, 4 °C) to separate out bacterial matter after incubating at 37 °C with stirring for 4 h. The particles were subsequently resuspended and subjected to a reaction with TBA to derivatize MDA to produce a coloured adduct. The samples were allowed to cool following incubation at 95 °C for 60 min and centrifuged (5000×rpm, 10 min) to get rid of cellular debris. Using 600 nm as the reference wavelength, the absorbance associated with the MDA-TBA adduct has been measured at 532 nm. With an extinction coefficient of 1.55×10^5 mM^{-1} cm^{-1}, MDA concentration was determined and expressed as nanomoles per millilitre (nmol/mL). Intracellular GSH levels, a critical antioxidant defence protein towards the effects of oxidative stress, are measured through a modified Ellman's method (Sedlak and Lindsay 1968). Bacterial cells treated with PtHGNM at their corresponding MICs for 4 h. The antibiotic ampicillin as well as a no-treatment control has been included for comparison as positive and negative controls. Cell aggregates were retrieved and rinsed with PBS to remove residual media, by centrifugation (10,000 rpm, 5 min, 4 °C). Proteins were eventually precipitated using a phenol-chloroform extraction. The ensuing aqueous phase, containing GSH, was subjected to incubation with 5,5′-dithiobis-(2-nitrobenzoic acid) (DTNB) for the production of a yellow coloured 2-nitro-5-thiobenzoate (TNB) anion, measurable at 412 nm using a spectrophotometer.

Briefly, bacterial cultures were treated for 6 h with PtHGNM at their respective MICs. Positive and negative control groups, ampicillin-treated and untreated cultures, were maintained. Then cells are extracted and washed twice to eradicate the residual media components by centrifugation at 10,000 rpm for 5 min at 4 °C and with PBS, following incubation. About 500 µL of PBS was added to resuspend the resulting cell aggregates. Catalase (CAT) activity relies on the enzymatic

rate of decomposition of hydrogen peroxide. The reaction mixture of 3 mL was prepared by adding 15-mM H_2O_2 solution to the cell suspension prepared in PBS. Catalase activity was measured by the decrease in H_2O_2 concentration at 240 nm. CAT activity was determined and expressed as unit/milligram protein (U/mg) (Yuan et al. 2017). The superoxide dismutase (SOD) activity assay relies on the enzymatic dismutation of superoxide radicals by SOD, which inhibits the photochemical reduction of nitro blue tetrazolium (NBT) to a coloured formazan product. The reaction mixture contained 63-mM NBT and 13-mM methionine, 1.3-mM riboflavin, 50-mM phosphate buffer (pH 7.0, for optimal activity) and cell suspension. The amount of reduced NBT; formazan was measured at 560 nm. SOD activity was determined and expressed as unit/millilitre (U/mL) (Yuan et al. 2017).

Statistical analysis

All experiments were carried out in triplicate, and the results are presented as error by mean ± standard deviation (SD). All experimental data were compared using Student's ***t-test — $P<0.01$, **t-test — $0.01<P<0.05$ and *t-test — $P>0.05$ which were considered statistically significant.

Results and discussion

Fabrication and characterization of PtHGNM

The filtered aqueous extract of *A. sativum* revealed the presence of a diverse phytochemical profile, including alkaloids, amino acids, flavonoids, phenols, reducing sugars, saponins, terpenoids, and triterpenoids. During the initial stage of nanoparticle synthesis, the reaction mixture constituting aqueous extract of snow mountain garlic and platinum metal precursor solution exhibited a characteristic opaque and golden yellow colour. Along the course of incubation, the solution became transparent with bright gold hue and a dense, brown brume resembling sediment formed at the bottom of the reaction vessel. The sediment observed likely due to phytocompounds involved in stabilization and surface capping of constituent elements of the nanoparticle accumulated, thereby facilitating their separation from the reaction medium. Subsequent centrifugation and drying of the pellet yielded approximately ~ 50 mg of crystalline like brown powder, i.e. platinum — Himalayan garlic nanoparticle (PtHGNM).

Synthesis of PtHGNM was examined using UV-visible spectroscopy by scanning across 210 and 800 nm. Surface plasmon resonance (SPR) peaked within the 210 to 300 nm range, with a maximum absorption intensity at 228 nm (Fig. 1a), consistent with studies reported for the formation of platinum nanomaterials

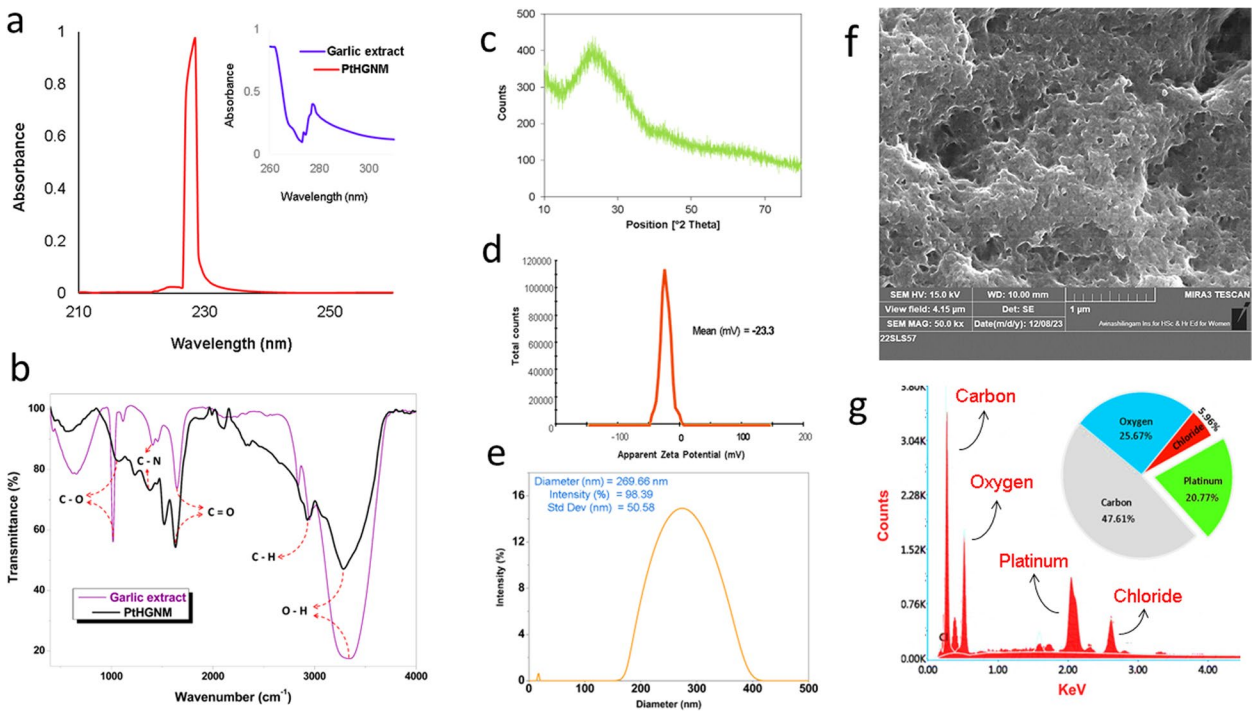

Fig. 1 Characterization of PtHGNM. **a** UV-visible spectrophotometric analysis. **b** FT-IR analysis of PtHGNM and Himalayan garlic extract. **c** XRD analysis. **d** Zeta-potential analysis. **e** Dynamic light scattering analysis. **f** FESEM image. **g** EDAX analysis of PtHGNM

(Herricks et al. 2004; Mendivil Palma et al. 2016; Taniguchi et al. 2019). The position and intensity of the SPR peak are size dependent. Maximum absorption detected at a lower wavelength (228 nm) stipulating the nanoscale size of the PtHGNM. Smaller particle size translates a weaker force of attraction of the conduction electrons towards the core, allowing them to excite at higher energy level upon absorption of light, i.e. photons (Tahir et al. 2017; Thongnopkun and Kitprapot 2021). This accounts for the really intense and well-defined narrow peak at 228 nm. UV-vis spectroscopy was also performed on the aqueous garlic extract for reference. The extract reached a maximum in its absorption spectrum at 277 nm, which designates the presence of sulphide compounds, particularly allicin (Prabakar and Akilan 2018). This absorption peak also falls within the range reported in previous studies (Ali et al. 2023).

Both the nanoparticle and Himalayan garlic (*A. sativum*) extract undergone for FT-IR analysis, and the spectrum was measured across 400 to 4000 cm^{-1}, to perceive about the functional groups and corelate potential biomolecules present in both phytocompounds and nanoparticles (Fig. 1b). This technique allowed us to characterize the functional groups present in the samples. Peaks at 3289 cm^{-1} in PtHGNM and 3328 cm^{-1} in the garlic extract were assigned to the O–H stretching vibration of alcohols. Peaks at 2927 cm^{-1} in PtHGNM and 2950 cm^{-1} in the extract indicated the presence of C–H stretching vibrations in alkanes. Peaks at 1630 cm^{-1} in PtHGNM and 1644 cm^{-1} in extract indicate C=O stretching vibrations of carbonyls. Peaks at 1384 cm^{-1} in PtHGNM and 1410 cm^{-1} in the extract indicated the vibrations of C–N. Finally, peaks at 1076 cm^{-1} in PtHGNM and 1014 cm^{-1} in the extract correspond to C–O stretching vibration of esters. The FTIR spectra showed shifts in the positions of some characteristic bands between the plant extract and the PtHGNM. These shifts suggest possible interactions between the functional groups of plant biomolecules and the surface of the nanoparticle. The functional groups also suggest the deposition of phytocompounds like flavonoids, without any chelating agents possibly interacted via π-electrons in the carbonyl groups. Oxidation of hydroxyl groups during the reduction and stabilizing of PtHGNM might have released oxidized forms, thereby initiating capping of the surface of the nanoparticles. With the presence of carbonyl, carboxylate and amine groups, it aids in hindering the nanoparticles from agglomeration and also stabilizes them (Megawati et al. 2023). The presence of these functional groups possibly acts as reducing agents during reduction reaction of Pt^{4+} ions to Pt^{0} nanoparticles and also might stabilize these nanoparticles.

In order to understand the constituent atoms nature of arrangement within the nanoparticle, X-ray diffraction (XRD) pattern analysis was performed. XRD profile exhibited a broad peak at roughly ~25 with 2θ value (Fig. 1c) referring to amorphous platinum (Ma et al. 2014). It produced no other peaks, and no peaks associated with crystalline platinum were intercepted, necessitating nanoparticulate and amorphous nature of PtHGNM (Wang et al. 2011, 2013; Nethravathi et al. 2011; Sun et al. 2007).

The charge disseminated around the nanoparticles was measured using zeta-potential analysis to define the degree of stabilization. The PtHGNM exhibited a negative zeta-potential value of −23.3 mV (Fig. 1d), indicating their exceptional colloidal stability. Since the magnitude of the zeta potential is directly correlated with electrostatic repulsion forces between nanoparticles, higher absolute values reveal greater repulsion and enhanced stability in suspension. The negative zeta potential indicated that the PtHGNM surface is covered with negatively charged moieties, likely derived from the plant extract, contributing to electrostatic repulsion between nanoparticles, to long-term stability and prevents aggregation. These results are also correlated with the FT-IR analysis, confirming the efficacy of the garlic extract in synthesis of platinum nanoparticles.

A particle size study of the platinum nanoparticles was inspected via size distribution by intensity method based on their supposed Brownian motion. The DLS analysis showed a maximum intensity of size distribution at 269 nm (Fig. 1e). Compared to the size predicted by the FESEM was quite larger since the FESEM imaging measures only along the X–Y plane and not along three dimensions like DLS. The reason attributed to the high value might be either due to hydrodynamic diameter, arisen by the biomolecules coated onto surface of the nanoparticle or alongside due to possible agglomerated portions within the sample. The polydispersity index (PDI) of 45.60% indicates a moderate degree of polydispersity.

Field emission scanning electron microscopic (FESEM) imaging technique was used to survey the surface topography, general appearance and morphology of the nanoparticles. The image (Fig. 1f) revealed a closely packed, aggregated structure with an extremely porous and a complex interlocked paradigm with a size ranging around 28 nm. This layered porous architecture with varying pore dimensions likely has a relatively larger surface area. The chemical makeup of the nanoparticles was also examined with EDAX analysis. It detected the presence of the platinum, carbon, oxygen and chloride elements and revealed their corresponding atomic values, roughly ~20, 47, 25 and 5% by weight (Fig. 1g).

In vitro toxicological effects of PtHGNM

Stringent evaluation of potential hazards to biological entities and the environment are necessary during the nanoparticle development. Toxicity assays, including both cytotoxicity and ecotoxicity, play a crucial role in this pursuit by evaluating potential environmental releases. There is a correlation between nanoparticle size, surface area, their ability to generate reactive oxygen species (ROS) and their overall toxicity, as proven in existing research (Yu et al. 2020). Our present study, specifically focused on teratogenic and phytotoxic effects, aims to contribute to this field by investigating the possible biological consequences of nanoparticle exposure.

Phytotoxic effects of PtHGNM on *V. radiata*

Studies have demonstrated that platinum ions, at lower concentrations, can promote seed germination and stimulate beneficial effects on plant growth. These positive effects include increased root length, leaf area, fresh mass, dry matter and photosynthetic activity. However, at higher concentrations, these same ions exhibit phytotoxic effects, hindering plant growth and development (Gawrońska et al. 2018). The exposure of PtHGNM to *V. radiata's* (mung bean) seed germination and its effects on their growth parameters were analysed in this study (Fig. 2a). At concentrations of 7.8, 15.6, 31.2 and 62.5 µg/mL, the germination rate was significantly enhanced by PtHGNM exposure compared to the control group, which exhibited an 88% germination rate. All PtHGNM-treated groups achieved a 100% germination rate (Fig. 2b).

We also evaluated *V. radiata's* growth parameters through measuring shoot length, root length and fresh mass to assess the impact of PtHGNM on seedling development following a 5-day exposure period significant increases which were observed in shoot length and fresh mass compared to the control (Fig. 2c, d, e). Specifically, there was an increase in the shoot length and fresh mass of PtHGNM-treated *V. radiata* seedlings by 6.91 cm and 0.09 g, respectively. Interestingly, root length displayed a concentration-dependent response. While lower treatment concentration (7.8 µg/mL) showed a trend of increased root length compared to the control, higher concentrations (15.6, 31.2 and 62.5 µg/mL) resulted in a decrease in root length, still greater than the control group when compared. This suggests a possible hormetic effect of PtHGNM on root development. Hormesis is a biphasic dose–response relationship where low doses elicit a stimulatory response, while high doses induce inhibition. Emerging evidence indicates widespread hormetic responses in plants when exposed to nanomaterials (Agathokleous et al. 2019). Nanoparticle applications hold promise for improving agricultural sustainability and security by modulating plant stress responses and potentially inducing hormetic effects in crops. It is achieved by interacting with and influencing one or more of the following: signalling molecules, phytohormones and nutrient uptake, ultimately leading to enhanced stress resilience (Rai et al. 2023). Metal ions are known

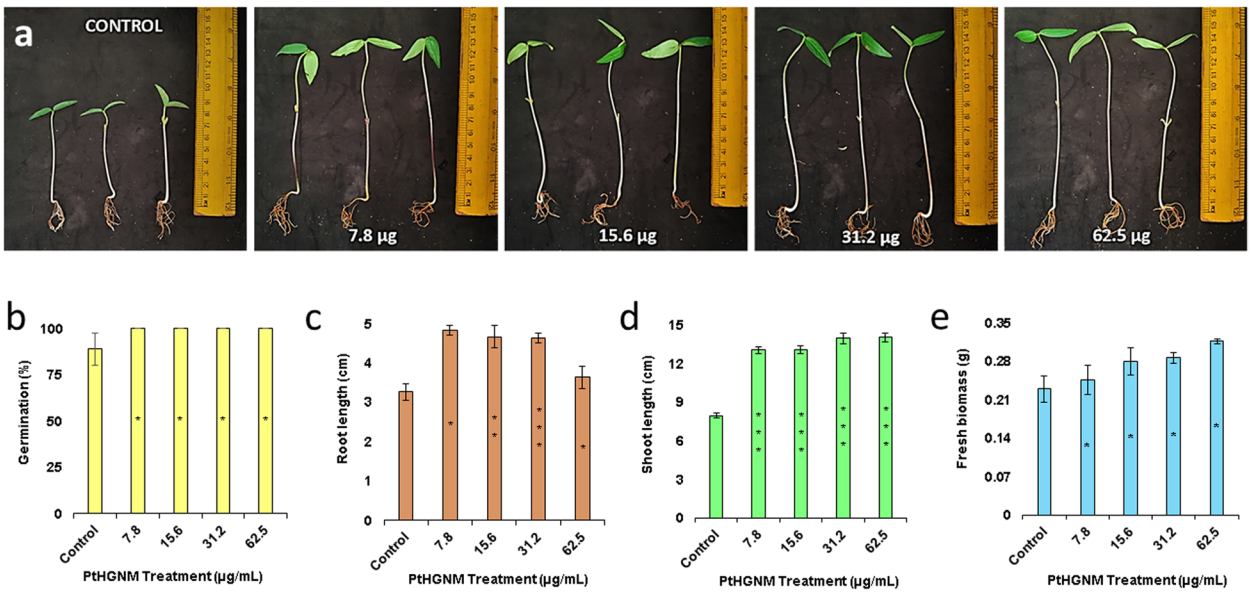

Fig. 2 *Vigna radiata* phytotoxicity analysis. **a** Qualitative and **b** quantitative analysis of seed germination. **c** Root length, **d** shoot length and **e** fresh biomass of *V. radiata* treated with PtHGNM

for inducing hormesis in plants (Jalal et al. 2021). While extensive research has focused on the detrimental effects of heavy metal (HM) toxicity on plants, the stimulatory potential of sub-toxic HM concentrations, i.e. hormesis, remains less explored. As mentioned earlier, studies with evidence for hormetic responses in plants demonstrated enhanced growth at low Cd exposures in *Lonicera japonica* (Jia et al. 2015) and *Brassica juncea* (Seth et al. 2008). Pb also showed stimulatory effects in *Arabis paniculata* (Tang et al. 2009) and corn (Figlioli et al. 2019). Lower concentrations of Cd and Pb have been reported to stimulate growth in corn, with documented increases in shoot biomass of up to 29% and 27% compared to controls (Małkowski et al. 2020). TiO_2 at lower concentrations also showed stimulatory effects in *Lemna minor* when compared to higher concentrations (Song et al. 2012). Similarly, platinum at lower concentrations showed beneficiary effects on exposure to *Arabidopsis thaliana* L. (Gawrońska et al. 2018). With the all evidence stating the beneficiary effect exhibited by the garlic platinum nanoparticles, it still remains unclear the mechanism of action of the nanoparticles. There is not much studies regarding how the platinum can impact and the mechanism of action on the plants either. Further investigations were required on the mechanism of the hermetic effect induced by the platinum nanoparticles. Studies associated with huge population samples and analysis of platinum's translocation, their effects on the plant's biochemical parameters, etc. are required to deduce the underlying process of the platinum metal.

Toxicological effects of PtHGNM on *D. rerio* embryos

During embryogenesis, being exposed to heavy metals can disrupt numerous aspects of development, resulting in a decline in the number and viability of the offspring. These abnormalities can be expressed as developmental malformations, preterm hatching, prolonged hatching or higher mortality among newly hatched embryos (Sfakianakis et al. 2015). Throughout the 96-h post-fertilization (hpf) period, untreated control embryos exhibited normal development with 0% mortality. PtHGNM did not impact embryo viability, with all embryos reaching 100% viability at all the test concentrations: 1, 5, 10, 20, 30, 40, 50 and 60 µg/mL and also resulted in normal development as well (Fig. 3a). PtHGNM exposure across all the test concentrations (1–60 µg/mL) caused a significant delay in hatching when compared to the control (Fig. 3b). With the reductions ranging from 6.67 to 20%, hatching was delayed by 48 hpf. It became partially pronounced around 72 hpf, with the reductions in hatching rates ranging around 13.33 to 40%. However, full hatching did achieve at 96 hpf. Notably, the nanoparticle concentration directly impacted the severity of the hatching delay, with higher concentrations leading to greater delays.

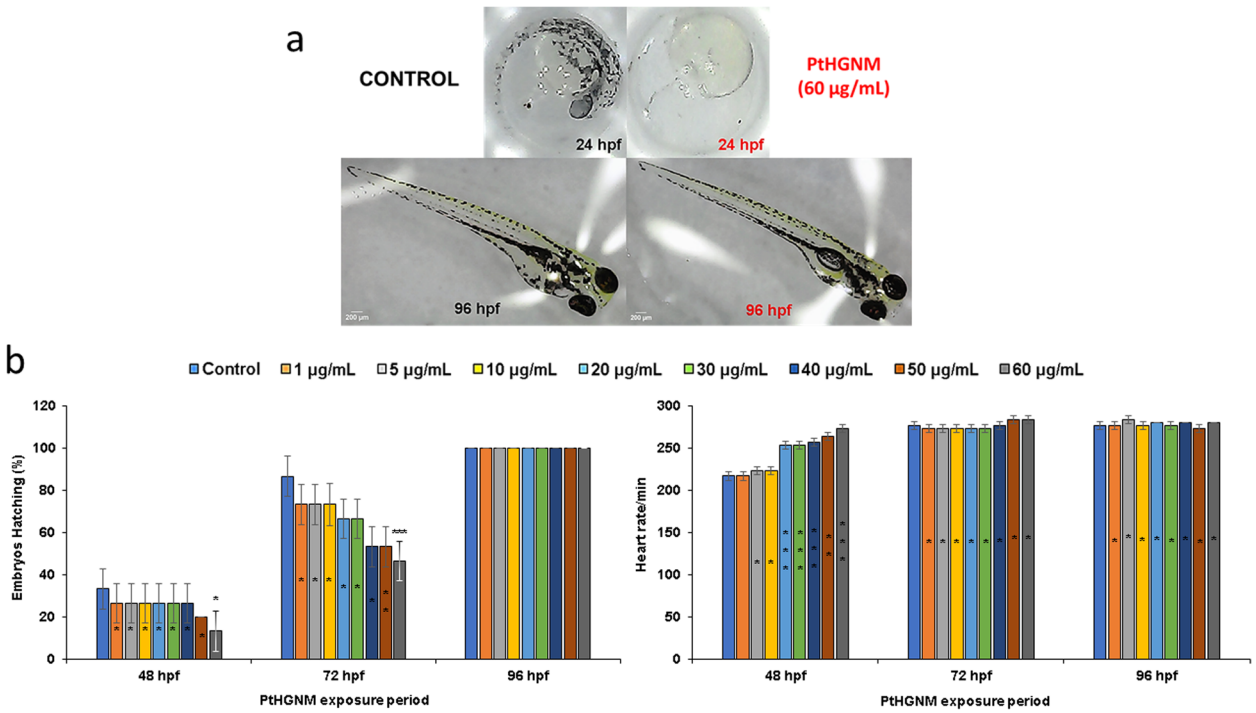

Fig. 3 Toxicity analysis of PtHGNM in *D. rerio* embryos. **a** Hatching of *D. rerio* embryos. **b** Hatching percentage and heart rate of *D. rerio* embryos exposed to PtHGNM

Furthermore, at 24 hpf, PtHGNM exposure induced chorionic fluid turbidity and a concentration-dependent decrease in the rate of embryonic development which were visible (Fig. 4b), when compared to control. This suggests early developmental processes are potentially impacted by PtHGNM and might be one of the potential causes of delayed hatching of the embryos observed.

Exposure to heavy metals results in increased heart rates in *D. rerio* (Taslima et al. 2022). Typically, zebrafish's heart beat (bpm) after 48 hpf would fall around 200 bpm (Gierten et al. 2020). A significant increase in heart rate (Fig. 3e) was induced when compared to the control group during the exposure to PtHGNM. A rise ranging from approximately 6 to 56 beats per minute (bpm) was first observed at 48 hpf when compared to control. The rise in heart rate continued at a slower pace at 72 hpf, with a less pronounced increase compared to 48 hpf. Interestingly, by 96 hpf, heart rate appeared to stabilize, with no significant difference observed between the control and PtHGNM-exposed groups, i.e. it falls between 273 and 283 bpm. Finally, to assess the potential neurodevelopmental effects of PtHGNM exposure, the larval touch response was evaluated. No significant decrease across all the test concentrations in touch response was observed. Results were also consistent with previously established study established using platinum nanoparticles (Asharani et al. 2011).

Despite the observed hatching delay, and chorionic fluid turbidity, PtHGNM exposure did not appear to influence other developmental parameters, including tail detachment from the yolk sac, heartbeat visibility at 48 hpf, somite formation and not induced any morphological abnormalities. A comprehensive analysis of the potential long-term effects on organogenesis and overall embryonic health of *D. rerio* with exposure to PtHGNM is required. Investigations with larger sample sizes and potentially using established quantitative behavioural assays are required to understand: Delayed development during embryonic phase, how the heart rates stabilized at 96 hpf indicating possible tolerance development to heavy metals and to elucidate the underlying mechanisms and potential long-term consequences. The results of our study highlight the potential risks associated with the in vivo utilization of Himalayan garlic-platinum nanoparticles, implying the possibility of similar ramifications. A cautious strategy is required when it comes to the dispersal of nano waste along with the application of nanoparticles in vivo, as this may result in indirect human exposure via substances, say fresh water fish, etc., contaminated with nanoparticles in effluent. These studies yield significant data that can be utilized in subsequent inquiries concerning the mechanisms underlying nanoparticle toxicity, an intricate field that demands ongoing research endeavours.

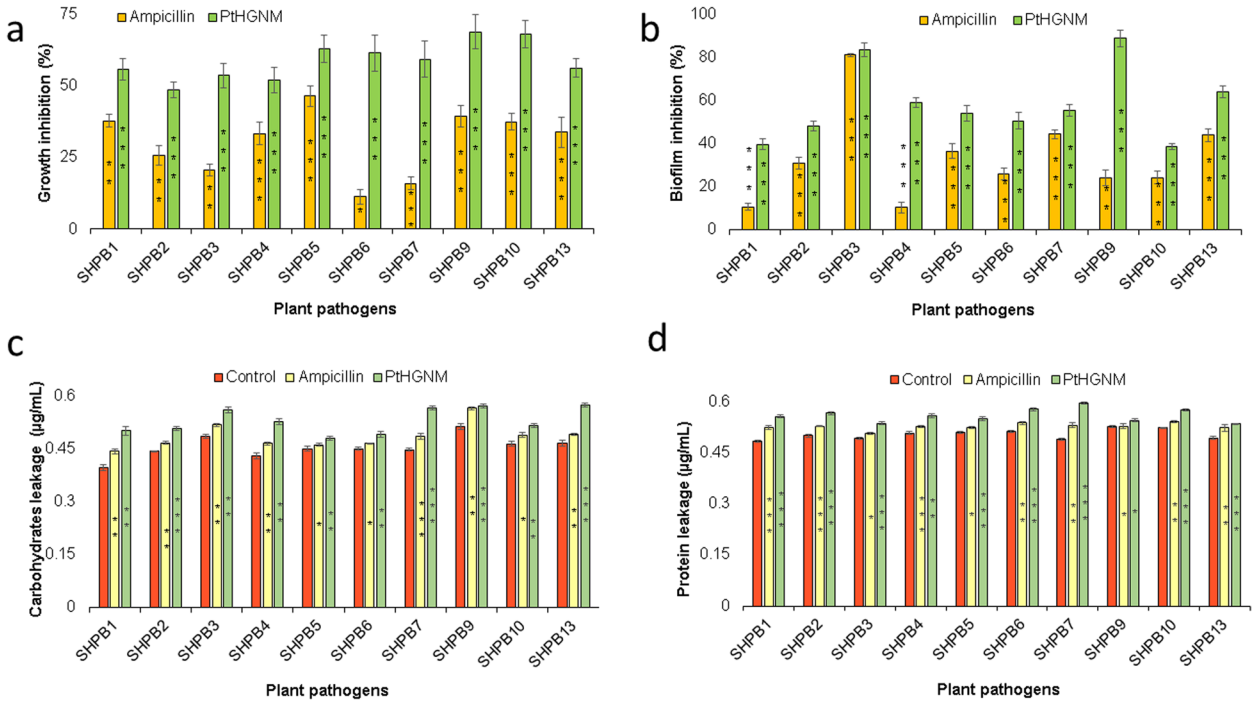

Fig. 4 Antibacterial activity of PtHGNM. **a** Growth inhibition. **b** Biofilm inhibition by PtHGNM in *Bacillus* sp. **c** Carbohydrates leakage and **d** protein leakage in *Bacillus* sp. treated with PtHGNM

Identification and evolutionary relationships of bacterial phytopathogens

Phytopathogens isolated were identified to be *Bacillus licheniformis* strain SHPB1 (MZ242758.1), *Bacillus subtilis* strain SHPB9 (MZ244204.1) and *Bacillus aerius* strain SHPB10 (MZ244207.1) from pepper plant, *Bacillus glycinifermentans* strain SHPB2 (MZ243088.1), *Bacillus sonorensis* strain SHPB3 (MZ243140.1), *Bacillus paralicheniformis* strain SHPB4 (MZ243215.1), and *Bacillus haynesii* strain SHPB5 (MZ243316.1) from coffee plant, *B licheniformis* strains SHPB6 (MZ243466.1), SHPB7 (MZ243467.1) and *B. paralicheniformis* strains SHPB13 (MZ244347.1) from cardamom plant. These plant pathogenic bacteria were served as model organisms for this study. Antibiotic susceptibility profiles were analysed, revealing diverse resistance patterns across species (Table 1).

The phylogenetic tree revealed the hypothesized relative closeness of the model organisms (Fig. S1a). Phylogenetic tree was also built for *B. licheniformis* strain SHPB1 (Fig. S1b), *B. glycinifermentans* strain SHPB2 (Fig. S1c), *B. sonorensis* strain SHPB3 (Fig. S1d), *B. paralicheniformis* strain SHPB4 (Fig. S2a), *B. haynesii* strain SHPB5 (Fig. S2b), *B. licheniformis* strains SHPB6 (Fig. S2c) and SHPB7 (Fig. S2d), *B. subtilis* strain SHPB9 (Fig. S3a), *B. aerius* strain SHPB10 (Fig. S3b), *B. paralicheniformis* strain SHPB13 (Fig. S3c) and their respective highly similar organisms identified. Figure S4 showed global relative relationship between all the similar organisms and the *Bacillus* spp. phytopathogens.

Antibacterial and antibiofilm activity of PtHGNM

A group of wells that did not indicate any signs of turbid development was selected for the MIC depiction. MIC was observed as (Fig. 4a and Table 2) 7.81 µg/ml for SHPB13 strain of B. paralicheniformis and SHPB3 strain of B. sonorensis, 15.62 µg/ml for SHPB4 strain of B. paralicheniformis, SHPB2 strain of B. glycinifermentans and SHPB1 strain of B. lichenifromis, 31.25 µg/ml for SHPB5 strain of B. haynesii, SHPB9 strain of B. subtilis, and SHPB10 strain of B. aerius, 62.5 µg/ml for SHPB6 and SHPB7 strains of B. lichenifromis. PtHGNM exposure resulted in 48–68% growth inhibition of the phytopathogens when compared to control

Table 1 Antibiogram for isolated *Bacillus* sp. phytopathogens

	Gentamicin	Amikacin	Ceftriaxone	Streptomycin	Cefoperazone	Kanamycin	Penicillin	Ampicillin	Cefepime
SHPB1	S	S	S	S	S	S	R	R	S
SHPB2	S	S	S	S	S	S	R	R	R
SHPB3	S	S	R	S	R	S	R	R	R
SHPB4	S	S	R	S	R	S	R	R	R
SHPB5	S	S	S	R	S	S	R	R	R
SHPB6	S	S	S	S	S	S	R	R	S
SHPB7	S	S	S	S	S	S	R	R	R
SHPB9	S	S	S	S	S	S	R	S	R
SHPB10	S	S	S	S	S	S	R	S	R
SHPB13	S	S	S	S	R	S	S	R	R

S Susceptible, *R* Resistant

Table 2 Minimum inhibitory concentration (MIC), minimum bactericidal concentration (MBC) and antibiofilm concentration (ABC) of PtHGNM for isolated *Bacillus* sp. phytopathogens

Strain	Species	Plant source	MIC (µg/mL)	MBC (µg/mL)	ABC (µg/mL)
SHPB1	*B. licheniformis*	Pepper	15.62	31.25	15.62
SHPB2	*B. glycinifermentans*	Coffee	15.62	31.25	31.25
SHPB3	*B. sonorensis*	Coffee	7.81	15.62	7.81
SHPB4	*B. paralicheniformis*	Coffee	15.62	15.62	31.25
SHPB5	*B. haynesii*	Coffee	31.25	31.25	62.5
SHPB6	*B. licheniformis*	Cardamom	62.5	62.5	62.5
SHPB7	*B. licheniformis*	Cardamom	62.5	62.5	62.5
SHPB9	*B. subtilis*	Pepper	31.25	62.5	62.5
SHPB10	*B. aerius*	Pepper	31.25	62.5	62.5
SHPB13	*B. paralicheniformis*	Cardamom	7.81	15.62	15.62

(***t-test — $P<0.01$, **t-test — $0.01<P<0.05$ and *t-test — $P>0.05$). MBC was evaluated (Table 2), and the findings indicated that ~ 15–65 µg/mL of PtHGNM can completely inhibit the growth and the colony formation of the selected plant-borne bacterial phytopathogens. Antibiofilm assay (Fig. 4b and Table 2) disclosed that ~ 7–65 µg/mL of PtHGNM was necessary and suppressed the biofilm formation by 34–88% when compared to the control (***t-test — $P<0.01$ and **t-test — $0.01<P<0.05$). The antibiofilm efficacy of ampicillin and PtHGNM against the tested bacterial strains exhibited varying degrees of inhibition. While ampicillin demonstrated moderate inhibitory effects, PtHGNM displayed a broader spectrum of activity, with significant biofilm reduction observed in several strains. These findings suggest that PtHGNM holds promise as a potential antibiofilm agent. However, the observed variations in biofilm inhibition among different bacterial strains highlight the complex nature of biofilm formation and the need for further investigation into the underlying mechanisms of action for both compounds.

Influence of PtHGNM on phytopathogens membrane integrity

As a marker of membrane permeability and damage, the release of cytoplasmic proteins and sugars was measured after treating the cultures with PtHGNM at their respective minimum inhibitory concentrations (MICs). The optical density values for both the sugars and proteins were found to be increased after the treatment with PtHGNM. Compared to the negative control, PtHGNM treatment resulted in a significant increase (***t-test — $P<0.01$ and **t-test — $0.01<P<0.05$) in the release of both proteins (approximately 0.1 µg/mL) and sugars (0.1–0.2 µg/mL) (Fig. 2c and d). Increase in cytoplasmic leakage of essential biomolecules, including proteins crucial for cellular function and sugar, which is the fundamental carbon source for organic molecules and acts as crucial cellular energy reservoir for the bacteria suggests that PtHGNM compromise bacterial membrane integrity. Cellular efflux of intracellular sugar exhibited a trend consistent with the proteins, indicating that PtHGNM's ability to disrupt the cell membrane. Additionally, the similarity in the release patterns of proteins and sugars implies that PtHGNM can induce non-specific membrane permeabilization, causing the leakage of both macromolecules and other solutes. The leakage was more evident, suggesting PtHGNM may accelerate the protein and sugar leakage from the bacterial cytoplasm after an extended duration of treatment. This potential mechanism for PtHGNM action warrants further investigation.

Influence of PtHGNM on phytopathogens antioxidant system

To evaluate the potential of PtHGNM to induce oxidative damage to cells, we examined the production of malondialdehyde (MDA), which is known as a common biomarker to measure the peroxidation of lipids. The quantification of MDA, an unstable aldehyde produced when reactive oxygen species (ROS) peroxidize polyunsaturated fatty acids, was measured on bacterial cultures that had been exposed to different concentrations of PtHGNM. Such reactions generate unsaturated aldehydes, which are associated with the dysfunctional and structural changes of different cellular elements, including proteins along with other macromolecules. A significant increase (***t-test — $p<0.01$, **t-test — $0.01<P<0.05$ and *t-test — $P>0.05$) in MDA levels (0.01–0.025 nmol/mL) was observed in PtHGNM-treated cultures when compared to untreated controls (Fig. 5a). This elevation in MDA content suggests that PtHGNM may trigger oxidative stress in bacteria, potentially contributing to their observed antibacterial effects. We further estimated GSH (glutathione) levels, to investigate the pro-oxidant potential of PtHGNM. By scavenging reactive oxygen species (ROS), GSH, a vital cytoplasmic thiol-containing tripeptide, has implications in preserving the cellular redox state (Liu et al. 2022b). Thereby, a decline in the level of GSH acts as an indication of elevated oxidative stress. As such, we hypothesized that PtHGNM treatment would alter GSH homeostasis. Following exposure to PtHGNM, cellular GSH levels were significantly reduced (***t-test — $P<0.01$, **t-test — $0.01<P<0.05$ and *t-test — $P>0.05$) by around 20–50%, when compared to untreated controls (Fig. 5b). This observed reduction in levels of GSH signifies that PtHGNM could trigger an oxidative stress response by facilitating the production of ROS and overwhelming the cellular antioxidant defence framework, possibly jeopardizing cell viability.

Platinum ions can induce the generation of reactive oxygen species (ROS), including hydroxyl radicals (OH), along with or without superoxide anions (O_2^-), via hydrogen peroxide (H_2O_2) decomposition (Serra-Maia et al. 2021). Thus, we did measure the activities of superoxide dismutase (SOD) and catalase (CAT) in bacterial cultures in response to ROS production to evaluate the potential impact of PtHGNM on the cellular antioxidant defence system. Antioxidant enzymes SOD and CAT are key enzymes that detoxify superoxide radicals and hydrogen peroxide, respectively. Cellular antioxidative response disruption induced by ROS generation was elucidated by measuring the enzyme activities of bacterial suspensions. Following exposure to PtHGNM at various concentrations, both catalase activity and superoxide dismutase were significantly

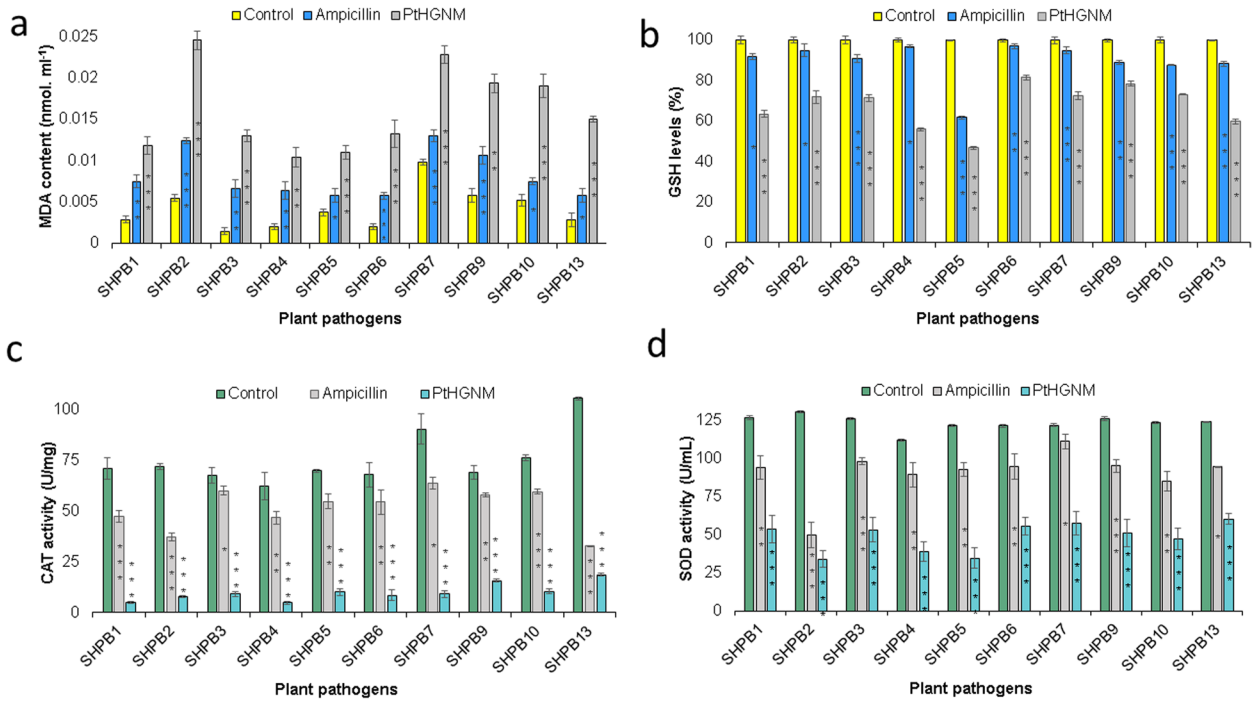

Fig. 5 Induction of oxidative stress by PtHGNM in *Bacillus* sp. Measurement of **a** malondialdehyde (MDA) and **b** glutathione (GSH) levels and **c** catalase (CAT) and **d** superoxide dismutase (SOD) enzyme activities in *Bacillus* sp. treated with PtHGNM

reduced (***t-test — $P < 0.01$, **t-test — $0.01 < P < 0.05$ and *t-test — $P > 0.05$) by around 52 to 88 (Fig. 5c) and 64 to 96 (Fig. 5d) enzymatic units when compared to untreated controls.

Collectively, our findings indicate that the PtHGNM exercise their antibacterial effects, if not solely in part, by eliciting a state of oxidative stress within bacterial cells. Rise in concentrations of MDA denotes a spike in lipid peroxidation, which is a signatory for oxidative degradation. The significant decrease in cellular GSH levels suggests a depletion of antioxidant defences. These combined alterations in oxidative stress markers likely contribute to the observed decrease in bacterial cell viability. Investigation also revealed that PtHGNM elicits antibacterial activity by generation of ROS, supposedly by reducing the activity of the antioxidant enzymes: CAT and SOD. Compromised antioxidant response could render bacteria more susceptible to oxidative stress, ultimately facilitate to their growth inhibition or death. Further investigations required to elucidate the precise mechanisms by which PtHGNM trigger ROS generation, to establish a correlation between observed changes in oxidative stress markers and bacterial growth inhibition and to establish conclusive evidence with other antibacterial mechanisms as well.

Conclusion

Utilizing *A. sativum* as a biological reducing agent highlights the potential for environmental sustainability and effective nanoparticle production. It also highlights the ingenuity of the metal nanoparticles as platinum Himalayan garlic nanoparticles (PtHGNM) hold tremendous potential as an antimicrobial agent, displaying notable efficacy in impeding the growth of harmful plant pathogens. The eco-friendly nature of their synthesis and their potent antimicrobial properties make PtHGNM ideal for sustainable plant disease management. The antimicrobial properties exhibited by these nanoparticles are highly promising and might not be limited only to combating plant diseases as focused in this study. This discovery, which dwells at the crossroads of nanotechnology, biotechnology, medicine, and agriculture, establishes a pathway towards a future of greener and more effective disease control.

Supplementary Information

The online version contains supplementary material available at https://doi.org/10.1186/s40712-024-00165-9.

Supplementary Material 1: Figure S1. a) Phylogenetic tree showing the relationship within the model organisms. Phylogenetic trees showing the relationship between b) *Bacillus licheniformis* strain SHPB1 c) *Bacillus*

glycinifermentans strain SHPB2 d) *Bacillus sonorensis* strain SHPB3 with their respective similar organisms. Figure S2. Phylogenetic trees showing the relationship between a) *Bacillus paralicheniformis* strain SHPB4 b) *Bacillus haynesii* strain SHPB5 c) *Bacillus licheniformis* strains SHPB6 and d) SHPB7 with their respective similar organisms. Figure S3. Phylogenetic trees showing the relationship between a) *Bacillus subtilis* strain SHPB9 b) *Bacillus aerius* strain SHPB10 and c) *Bacillus paralicheniformis* strain SHPB13 with their respective similar organisms. Figure S4. Phylogenetic tree showing global relationship between the model organismsand all the similar organisms identified.

Acknowledgements
Authors are thankful to B. S. Abdur Rahman Institute of Science & Technology, Chennai, for providing research facilities in the School of Life Sciences.

Authors' contributions
SH conceived and designed research. DK and SR conducted experiments. SH analysed data. All authors wrote the manuscript. All authors read and approved the manuscript.

Funding
Nil.

Availability of data and materials
The datasets used and/or analysed during the current study are available from the corresponding author on reasonable request.

Declarations

Competing interests
The authors declare that they have no competing interests.

Received: 12 June 2024 Accepted: 17 August 2024
Published online: 10 September 2024

References

Agathokleous E, Feng Z, Iavicoli I, Calabrese EJ (2019) The two faces of nanomaterials: a quantification of hormesis in algae and plants. Environ Int 131:105044. https://doi.org/10.1016/j.envint.2019.105044

Ali IAM, Ahmed AB, Al-Ahmed HI (2023) Green synthesis and characterization of silver nanoparticles for reducing the damage to sperm parameters in diabetic compared to metformin. Sci Rep 13(1):2256. https://doi.org/10.1038/s41598-023-29412-3

Anwar N, Mehmood A, Ahmad KS, Hussain K (2021) Biosynthesized silver nanoparticles induce phytotoxicity in *Vigna radiata* L. Physiol Mol Biol Plants 27(9):2115–2126. https://doi.org/10.1007/s12298-021-01073-4

Asharani PV, Lianwu Y, Gong Z, Valiyaveettil S (2011) Comparison of the toxicity of silver, gold and platinum nanoparticles in developing zebrafish embryos. Nanotoxicology 5(1):43–54. https://doi.org/10.3109/17435390.2010.489207

Behzad F, Naghib SM, Kouhbanani MAJ, Tabatabaei SN, Zare Y, Rhee KY (2021) An overview of the plant-mediated green synthesis of noble metal nanoparticles for antibacterial applications. J Ind Eng Chem 94:92–104. https://doi.org/10.1016/j.jiec.2020.12.005

Chopra H, Bibi S, Singh I, Hasan MM, Khan MS, Yousafi Q, Baig AA, Rahman MdM, Islam F, Emran T. Bin, Cavalu S (2022) Green metallic nanoparticles: biosynthesis to applications. Front Bioeng Biotechnol 10:874742. https://doi.org/10.3389/fbioe.2022.874742

El Shafey AM (2020) Green synthesis of metal and metal oxide nanoparticles from plant leaf extracts and their applications: a review. Green Process Synth 9(1):304–339. https://doi.org/10.1515/gps-2020-0031

Eltaweil AS, Fawzy M, Hosny M, Abd El-Monaem EM, Tamer TM, Omer AM (2022) Green synthesis of platinum nanoparticles using Atriplex halimus leaves for potential antimicrobial, antioxidant, and catalytic applications. Arab J Chem 15(1):103517. https://doi.org/10.1016/j.arabjc.2021.103517

Faisal S, Tariq MH, Abdullah, Zafar S, Un Nisa Z, Ullah R, Ur Rahman A, Bari A, Ullah K, Khan RU (2024) Bio synthesis, comprehensive characterization, and multifaceted therapeutic applications of BSA-resveratrol coated platinum nanoparticles. Sci Rep 14(1):7875. https://doi.org/10.1038/s41598-024-57787-4

Figlioli F, Sorrentino MC, Memoli V, Arena C, Maisto G, Giordano S, Capozzi F, Spagnuolo V (2019) Overall plant responses to Cd and Pb metal stress in maize: growth pattern, ultrastructure, and photosynthetic activity. Environ Sci Pollut Res 26(2):1781–1790. https://doi.org/10.1007/s11356-018-3743-y

Gautam A, Komal P, Gautam P, Sharma A, Kumar N, Jung JP (2021) Recent trends in noble metal nanoparticles for colorimetric chemical sensing and micro-electronic packaging applications. Metals 11(2):329. https://doi.org/10.3390/met11020329

Gawrońska H, Przybysz A, Szalacha E, Pawlak K, Brama K, Miszczak A, Stankiewicz-Kosyl M, Gawroński SW (2018) Platinum uptake, distribution and toxicity in Arabidopsis thaliana L. plants. Ecotoxicol Environ Saf 147:982–989. https://doi.org/10.1016/j.ecoenv.2017.09.065

Gierten J, Pylatiuk C, Hammouda OT, Schock C, Stegmaier J, Wittbrodt J, Gehrig J, Loosli F (2020) Automated high-throughput heartbeat quantification in medaka and zebrafish embryos under physiological conditions. Sci Rep 10(1):2046. https://doi.org/10.1038/s41598-020-58563-w

Harborne JB (1973) Phytochemical methods. Chapman and Hall, London, pp 1–32

Heath RL, Packer L (1968) Photoperoxidation in isolated chloro-plasts. I. Kinetics and stoichiometry of fatty acid peroxidation. Arch Biochem Biophys 125(1):180–198

Herricks T, Chen J, Xia Y (2004) Polyol synthesis of platinum nanoparticles: control of morphology with sodium nitrate. Nano Lett 4(12):2367–2371. https://doi.org/10.1021/nl048570a

Jalal A, de Oliveira Junior JC, Ribeiro JS, Fernandes GC, Mariano GG, Trindade VDR, dos Reis AR (2021) Hormesis in plants: physiological and biochemical responses. Ecotoxicol Environ Saf 207:111225. https://doi.org/10.1016/j.ecoenv.2020.111225

Jan H, Gul R, Andleeb A, Ullah S, Shah M, Khanum M, Ullah I, Hano C, Abbasi BH (2021) A detailed review on biosynthesis of platinum nanoparticles (PtNPs), their potential antimicrobial and biomedical applications. J Saudi Chem Soc 25(8):101297. https://doi.org/10.1016/j.jscs.2021.101297

Jia L, Liu Z, Chen W, Ye Y, Yu S, He X (2015) Hormesis effects induced by cadmium on growth and photosynthetic performance in a hyperaccumulator, Lonicera japonica Thunb. J Plant Growth Regul 34(1):13–21. https://doi.org/10.1007/s00344-014-9433-1

Kaningini AG, Nelwamondo AM, Azizi S, Maaza M, Mohale KC (2022) Metal nanoparticles in agriculture: a review of possible use. Coatings 12(10):1586. https://doi.org/10.3390/coatings12101586

Kaur B, Kumar N, Patel MK, Chopra K, Saxena S (2023) Validation of traditional claims of anti-arthritic efficacy of trans-Himalayan Snow Mountain garlic (*Allium ampeloprasum* L.) extract using adjuvant-induced arthritis rat model: a comparative evaluation with normal garlic (*Allium sativum* L.) and dexamethasone. J Ethnopharmacol 303:115939. https://doi.org/10.1016/j.jep.2022.115939

Liu S, Zhang Q, Li H, Qiu Z, Yu Y (2022a) Comparative assessment of the antibacterial efficacies and mechanisms of different tea extracts. Foods 11(4):620. https://doi.org/10.3390/foods11040620

Liu T, Sun L, Zhang Y, Wang Y, Zheng J (2022) Imbalanced GSH/ROS and sequential cell death. J Biochem Mol Toxicol 36(1):e22942. https://doi.org/10.1002/jbt.22942

Ma Y, Wang H, Li H, Key J, Ji S, Wang R (2014) Synthesis of ultrafine amorphous PtP nanoparticles and the effect of PtP crystallinity on methanol oxidation. RSC Adv 4(40):20722–20728. https://doi.org/10.1039/C4RA01973C

Małkowski E, Sitko K, Szopiński M, Gieroń Ż, Pogrzeba M, Kalaji HM, Zieleźnik-Rusinowska P (2020) Hormesis in plants: the role of oxidative stress, auxins and photosynthesis in corn treated with Cd or Pb. Int J Mol Sci 21(6):2099. https://doi.org/10.3390/ijms21062099

Malode U, Patil YS, Selokar YN, Yadav PR, Bhagat RP, Nikose VM, Thakare RU, Nimbarte S (2023) Sustainable approaches for the synthesis of biogenic platinum nanoparticles. Bull Natl Res Cent 47(1):130. https://doi.org/10.1186/s42269-023-01104-y

Megawati E, Bangun H, Putra I, Rusda M, Syahrizal D, Jusuf N, Eyanoer P, Lubis R, Amin M (2023) Phytochemical analysis by FTIR of Zanthoxylum acanthopodium, DC fruit ethanol extract, N-hexan, ethyl acetate and water

fraction. Med Arch 77(3):183. https://doi.org/10.5455/medarh.2023.77.183-188
Mehra R, Jasrotia RS, Mahajan A, Sharma D, Iquebal MA, Kaul S, Dhar MK (2020) Transcriptome analysis of Snow Mountain garlic for unraveling the organosulfur metabolic pathway. Genomics 112(1):99–107. https://doi.org/10.1016/j.ygeno.2019.07.014
Mendivil Palma MI, Krishnan B, Rodriguez GAC, Das Roy TK, Avellaneda DA, Shaji S (2016) Synthesis and properties of platinum nanoparticles by pulsed laser ablation in liquid. J Nanomater 2016:1–11. https://doi.org/10.1155/2016/9651637
Nethravathi C, Anumol EA, Rajamathi M, Ravishankar N (2011) Highly dispersed ultrafine Pt and PtRu nanoparticles on graphene: formation mechanism and electrocatalytic activity. Nanoscale 3(2):569–571. https://doi.org/10.1039/C0NR00664E
Pandit C, Roy A, Ghotekar S, Khusro A, Islam MN, Emran TB, Lam SE, Khandaker MU, Bradley DA (2022) Biological agents for synthesis of nanoparticles and their applications. J King Saud Univ Sci 34(3):101869. https://doi.org/10.1016/j.jksus.2022.101869
Prabakar K, Akilan S (2018) Spectral studies and antibacterial activity of garlic (Allium sativum L.). Int J Emerg Technol Innov Res 5(7):452–457
Rai PK, Song H, Kim K-H (2023) Nanoparticles modulate heavy-metal and arsenic stress in food crops: hormesis for food security/safety and public health. Sci Total Environ 902:166064. https://doi.org/10.1016/j.scitotenv.2023.166064
Ranjani S, Shariq Ahmed M, Ruckmani K, Hemalatha S (2020) Green nanocolloids control multi drug resistant pathogenic bacteria. J Cluster Sci 31(4):861–866. https://doi.org/10.1007/s10876-019-01694-6
Salem SS, Fouda A (2021) Green synthesis of metallic nanoparticles and their prospective biotechnological applications: an overview. Biol Trace Elem Res 199(1):344–370. https://doi.org/10.1007/s12011-020-02138-3
Sedlak J, Lindsay RH (1968) Estimation of total, protein-bound, and nonprotein sulfhydryl groups in tissue with Ellman's reagent. Anal Biochem 25:192–205. https://doi.org/10.1016/0003-2697(68)90092-4
Serra-Maia R, Rimstidt JD, Michel FM (2021) Kinetic effect of surface chemisorbed oxygen on platinum-catalyzed hydrogen peroxide decomposition. Catal Lett 151(1):138–146. https://doi.org/10.1007/s10562-020-03280-2
Seth CS, Kumar Chaturvedi P, Misra V (2008) The role of phytochelatins and antioxidants in tolerance to Cd accumulation in Brassica juncea L. Ecotoxicol Environ Saf 71(1):76–85. https://doi.org/10.1016/j.ecoenv.2007.10.030
Sfakianakis DG, Renieri E, Kentouri M, Tsatsakis AM (2015) Effect of heavy metals on fish larvae deformities: a review. Environ Res 137:246–255. https://doi.org/10.1016/j.envres.2014.12.014
Song G, Gao Y, Wu H, Hou W, Zhang C, Ma H (2012) Physiological effect of anatase TiO_2 nanoparticles on *Lemna minor*. Environ Toxicol Chem 31(9):2147–2152. https://doi.org/10.1002/etc.1933
Soundhararajan R, Veerasami M, Khan S, Islam A, Srinivasan H (2023) Polyherbal nano formulation: a potent antibiotic resistance breaker in bovine mastitis causing MDR pathogens. J Mol Liq 392:123477. https://doi.org/10.1016/j.molliq.2023.123477
Sun Y, Zhuang L, Lu J, Hong X, Liu P (2007) Collapse in crystalline structure and decline in catalytic activity of Pt nanoparticles on reducing particle size to 1 nm. J Am Chem Soc 129(50):15465–15467. https://doi.org/10.1021/ja076177b
Tahir K, Nazir S, Ahmad A, Li B, Khan AU, Khan ZUH, Khan FU, Khan QU, Khan A, Rahman AU (2017) Facile and green synthesis of phytochemicals capped platinum nanoparticles and in vitro their superior antibacterial activity. J Photochem Photobiol B 166:246–251. https://doi.org/10.1016/j.jphotobiol.2016.12.016
Tang Y-T, Qiu R-L, Zeng X-W, Ying R-R, Yu F-M, Zhou X-Y (2009) Lead, zinc, cadmium hyperaccumulation and growth stimulation in Arabis paniculata Franch. Environ Exp Bot 66(1):126–134. https://doi.org/10.1016/j.envexpbot.2008.12.016
Taniguchi K, Shinoda K, Cuya Huaman JL, Yokoyama S, Uchikoshi M, Matsumoto T, Suzuki K, Miyamura H, Jeyadevan B (2019) Designed synthesis of highly catalytic Ni–Pt nanoparticles for fuel cell applications. SN Appl Sci 1(1):124. https://doi.org/10.1007/s42452-018-0133-5
Taslima K, Al-Emran M, Rahman MS, Hasan J, Ferdous Z, Rohani MF, Shahjahan M (2022) Impacts of heavy metals on early development, growth and reproduction of fish – a review. Toxicol Rep 9:858–868. https://doi.org/10.1016/j.toxrep.2022.04.013
Terán-Figueroa Y, de Loera D, Toxqui-Terán A, Montero-Morán G, Saavedra-Leos MZ (2022) Bromatological analysis and characterization of phenolics in Snow Mountain garlic. Molecules 27(12):3712. https://doi.org/10.3390/molecules27123712
Thongnopkun P, Kitprapot W (2021) Synthesis of the platinum particle with the pH variation for the particle size control. J Phys Conf Ser 2145(1):012038. https://doi.org/10.1088/1742-6596/2145/1/012038
Vijayaram S, Razafindralambo H, Sun Y-Z, Vasantharaj S, Ghafarifarsani H, Hoseinifar SH, Raeeszadeh M (2024) Applications of green synthesized metal nanoparticles — a review. Biol Trace Elem Res 202(1):360–386. https://doi.org/10.1007/s12011-023-03645-9
Wang H, Zhang X, Wang R, Ji S, Wang W, Wang Q, Lei Z (2011) Amorphous CoSn alloys decorated by Pt as high efficiency electrocatalysts for ethanol oxidation. J Power Sources 196(19):8000–8003. https://doi.org/10.1016/j.jpowsour.2011.05.062
Wang H, Ji S, Wang W, Wang R (2013) Amorphous Pt@PdCu/CNT catalyst for methanol electrooxidation. S Afr J Chem 66:17–20
Yu Z, Li Q, Wang J, Yu Y, Wang Y, Zhou Q, Li P (2020) Reactive oxygen species-related nanoparticle toxicity in the biomedical field. Nanoscale Res Lett 15(1):115. https://doi.org/10.1186/s11671-020-03344-7
Yuan Y-G, Peng Q-L, Gurunathan S (2017) Effects of silver nanoparticles on multiple drug-resistant strains of Staphylococcus aureus and Pseudomonas aeruginosa from mastitis-infected goats: an alternative approach for antimicrobial therapy. Int J Mol Sci 18(3):569. https://doi.org/10.3390/ijms18030569

Publisher's Note